Spatially resolved characterization of Xe ion irradiated LiF crystals using static field gradient NMR

2008 J. Phys.: Condens. Matter 20 465215

(http://iopscience.iop.org/0953-8984/20/46/465215)

J. Phys.: Condens. Matter **20** (2008) 465215 (6pp) doi:10.1088/0953-8984/20/46/465215

Spatially resolved characterization of Xe ion irradiated LiF crystals using static field gradient NMR

H Stork[1], K-P Dinse[2], F Fujara[1], A Hamburger[1], P Jakes[2], R Neumann[3], B Schuster[1,3], K Schwartz[3] and C Trautmann[3]

[1] Institut für Festkörperphysik, TU Darmstadt, Hochschulstraße 6, 64289 Darmstadt, Germany
[2] Eduard-Zintl-Institut für Anorganische und Physikalische Chemie, TU Darmstadt, Petersenstraße 18-20, 64287 Darmstadt, Germany
[3] Gesellschaft für Schwerionenforschung (GSI), 64291 Darmstadt, Germany

Received 7 August 2008, in final form 25 September 2008
Published 21 October 2008
Online at stacks.iop.org/JPhysCM/20/465215

Abstract
Spatially resolved ^{19}F and ^{7}Li nuclear magnetic resonance (NMR) spin–lattice relaxation rates have been measured in LiF crystals irradiated with 1.44 GeV Xe ions at fluences from 10^{10} to 10^{12} ions cm^{-2}. In addition, the F-centre concentration has been measured by optical absorption spectroscopy and the concentration of paramagnetic centres by electron paramagnetic resonance (EPR). Within the ion range, the relaxation rate turns out to increase linearly with the concentration of paramagnetic centres but super-linearly with the F-centre concentration. Beyond the ion range, the relaxation rate is still significantly enhanced compared to non-irradiated LiF.

1. Introduction

Quite recently, we proposed a NMR microimaging concept [1] which allows for the measurement of one-dimensional spatially resolved ^{19}F spin–lattice relaxation rate profiles. A resolution of the order of about 10 μm has been achieved in a LiF crystal irradiated with high-energy U ions. Technical aspects of the use of large static magnetic field gradients have been discussed as well as a special data acquisition mode allowing for effectively measuring spatially resolved spin–lattice relaxation rates as low as 10^{-3} s^{-1}.

The present work has now applied this concept to a detailed study of point defects in a series of LiF crystals being irradiated by high-energy Xe ions of varying fluences. For a short overview of the diverse experimental methods for detecting radiation induced defects in ionic crystals we refer to the references given in [1]. Here, we rather focus on magnetic resonance studies. There have indeed been previous NMR and EPR experiments on heavy ion irradiated LiF crystals [2, 3], but with the exception of our recently proposed approach [1] no spatial resolution had been attempted so far. Instead, in those studies [2, 3] the samples were irradiated by ions of sufficiently high energy such that no defect density gradient could be expected along the ion path direction. Their finding of a nuclear (^{19}F and ^{7}Li) spin–lattice relaxation rate T_1^{-1}, being related in a well defined way to the ion fluence, was interpreted in terms of F-centres acting as strong relaxation sinks, and the nuclear magnetization transport towards these centres was due to nuclear spin diffusion [4, 5].

2. Experimental details

LiF single crystals were irradiated by 1.44 GeV ^{130}Xe ions at the UNILAC linear accelerator of GSI Darmstadt, the ion fluences ranging from 10^{10} to 10^{12} ions cm^{-2}. During irradiation the beam current was monitored with a secondary electron emitting Al-foil detector which was calibrated by a Faraday cup leading to a fluence accuracy of about 20%.

The mean electron energy loss of the ions was 16.5 keV nm^{-1} and their penetration, also called ion range (R), was about 87 μm. The thickness of the LiF crystals was always larger than R.

The spatially resolved NMR experiments were carried out at a magnetic field of 3.74 T and a static magnetic field gradient of 74.3 T m^{-1}. The resonant nuclei were ^{19}F (149.6 MHz) and (to a lesser extent) ^{7}Li (61.8 MHz). The experimental temperature was set to (295 $\pm$ 2) K for all samples. In the case of ^{19}F-NMR, rf pulse lengths of 55 and 38 μs corresponding to thicknesses of the excited slice between 6 and

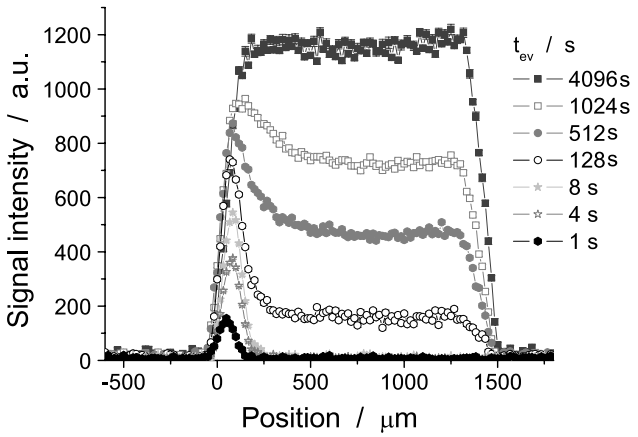

Figure 1. Selected evolution time (t_{ev}) weighted one-dimensional ^{19}F-NMR microimages of a Xe (incident energy 1.44 GeV, fluence of 10^{11} ions cm^{-2}) irradiated LiF crystal.

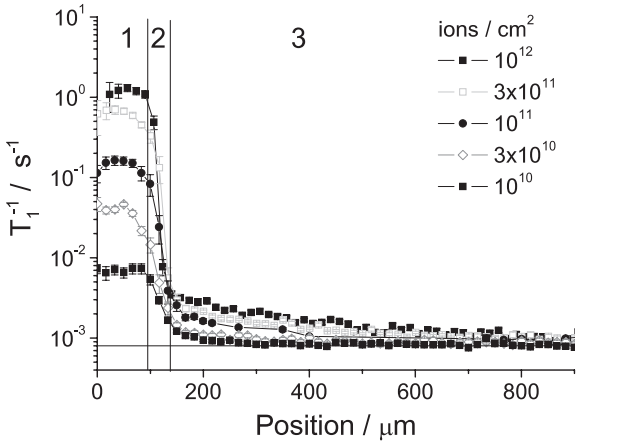

Figure 2. Position dependent ^{19}F spin–lattice relaxation rates for the Xe irradiated LiF crystals for several fluences, as noted in the inset. Three regions are marked: within the ion range (1), a transition region (2) and the deep crystal interior beyond the ion range (3). The horizontal line marks the spin–lattice relaxation rate of the non-irradiated sample.

8.5 μm, respectively, were applied. For the ^{7}Li experiments rf pulses 55–70 μs in length leading to slice thicknesses of 12–15 μm were used. A detailed description of our experimental procedure can be found in [1].

The NMR measurements were complemented by optical absorption spectroscopy and by multi-frequency EPR. The optical absorption experiments were carried out at room temperature using a UV–vis spectrometer (UNICAM) in the wavelength regime of 200–800 nm. The area density of the ion induced F-centres (N_F, in units of cm^{-2}) is deduced using the Smakula–Dexter formula (oscillator strength $f_F = 0.6$ [6, 7]) $N_F = 9.48 \times 10^{15} D_{opt}$, where D_{opt} is the optical density at the absorption maximum ($\lambda_{max} = 248$ nm). The accuracy of the optical density measurements was $\pm 2\%$. The F-centre concentration in the irradiated samples (n_F, in units of cm^{-3}) is equal to $n_F = N_F/R$.

The EPR experiments were performed using a commercial X-band (9.4 GHz) spectrometer (BRUKER ESP 300E) equipped with a rectangular cavity and a helium flow cryostat (Oxford). From the X-band (9.4 GHz) CW EPR experiments, carried out at 100 and 300 K, we obtained the integrated paramagnetic susceptibility and thus the total concentration of paramagnetic centres. For this determination the EPR spectra were background corrected using MnO as reference.

In addition, high-frequency (406.4 GHz) EPR spectra were recorded to probe for additional signals, which might not be resolved in the X-band spectra. The high-frequency EPR data were collected using the transmission-type EPR spectrometer at the National High Magnetic Field Laboratory (Tallahassee, USA). In this spectrometer the sample is mounted in the path of the microwave beam of approximately 6 mm diameter. Resonant absorption by paramagnetic centres is detected with a bolometer. The magnetic field of the superconducting magnet can be varied from 0 to 15 T, and narrow range sweeps with improved accuracy and field resolution can be performed with a superconducting sweep coil after switching the main coil to persistent mode. Although a quantitative determination of the number of paramagnetic centres has not been achieved, relative changes in absorption can be determined quite reliably ($\pm 30\%$) since samples of similar size were mounted at the same beam positions. The sample temperature can be varied from 4 to 300 K using a helium flow cryostat.

3. Results and discussion

3.1. Spatially resolved spin–lattice relaxation rates

Figure 1 exemplifies some spatially resolved ^{19}F signal intensity profiles of a LiF sample after Xe irradiation. First, the magnetization is destroyed, then the evolution time, t_{ev}, must elapse before determining the signal intensity. The figure indicates that only after sufficiently long evolution times, when all ^{19}F-spins are fully relaxed, is the true one-dimensional crystal profile found. For shorter evolution times the relaxation weighted image gradually changes such that it eventually represents only the irradiated part of the crystal.

From these evolution time weighted data one can deduce, in a straightforward manner, position dependent relaxation rates T_1^{-1}. This was done for all available LiF samples, irradiated with different fluences (figure 2). There is some ambiguity in assigning the zero position, i.e. the crystal surface. Here, the zero position is pragmatically defined by demanding that the fully relaxed signal intensity reaches 25% of the maximum intensity.

In the relaxation profiles, three regions, denoted by 1, 2 and 3, can be distinguished from each other. The nominally irradiated area (region 1), within $R = 87$ μm [8], can easily be identified by mono-exponential magnetization recovery curves yielding a high relaxation rate. There follows a transition zone (region 2) of approximately 50 μm thickness, where the relaxation rates decrease rapidly with increasing depth. In this transition region the magnetization decay curves have pronounced multi-exponential contributions (figure 3). Therefore, the mono-exponential model fits the data only poorly, which is reflected in figure 2 by the increased error

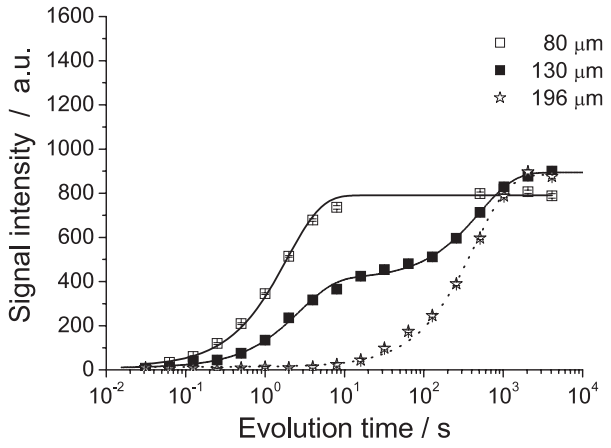

Figure 3. ^{19}F magnetization recovery curves in a LiF sample irradiated with 3×10^{11} Xe ions cm^{-2} at positions 80, 130 and 196 μm (cf figure 2). The fit curves for positions 80 and 196 μm are mono-exponential with $T_1 = 1.9$ s $\pm$ 0.1 s at 80 μm and $T_1 = 439$ s $\pm$ 19 s at 196 μm. At position 130 μm the signal intensity curve is fitted bi-exponentially with $T_1^a = 2.7$ s $\pm$ 0.2 s and $T_1^b = 515$ s $\pm$ 78 s.

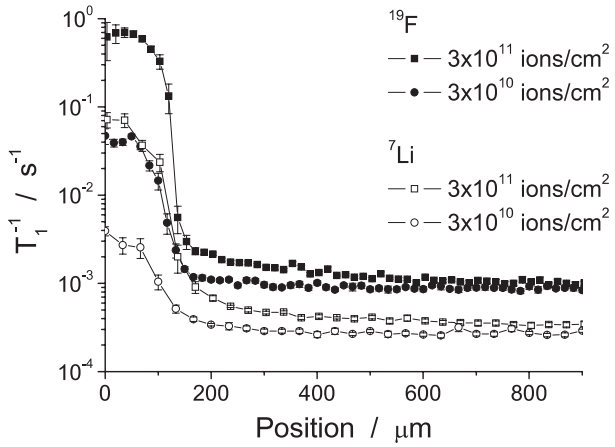

Figure 4. Comparison of the ^{19}F- and the ^{7}Li-relaxation rate profiles of two samples, irradiated at different Xe ion fluences. The assignment of the symbols is given in the inset. Note the different Larmor frequencies of ^{19}F (149.6 MHz) and of ^{7}Li (61.8 MHz).

bars in the transition region. Since R is well defined (the longitudinal beam straggling <3 μm [8]), we have to conclude that the width of the transition region is caused by a poorly defined crystal surface and random or systematic misalignment of the sample. This is supported by the edge width of the signal intensity profile of the fully relaxed sample (figure 1), and it also explains the high relative error at positions of less than 30 μm from the outer surface as being due to the smaller signal size at those positions. In region 3, beyond the transition range, the magnetization recovery curves are found to be mono-exponential again. Most remarkably, in this regime we still find a significantly enhanced spin–lattice relaxation rate. With increasing distance from region 1 this enhanced relaxation rate gradually decreases towards the background relaxation rate of the non-irradiated sample.

3.2. Comparison of ^{19}F and ^{7}Li relaxation rates

The samples irradiated with fluences of 3×10^{10} and 3×10^{11} ions cm^{-2} were also subjected to measurements of the ^{7}Li spin–lattice relaxation rate. In figure 4 we compare ^{7}Li with ^{19}F relaxation rates. For a given fluence, the ^{7}Li rate turns out to be always below the ^{19}F rate—by an order of magnitude within the ion range and by a factor of three beyond. Nevertheless, also in the ^{7}Li relaxation rate profiles, the same regions as in the ^{19}F relaxation rate profiles can be identified. Also the relaxation rate gradient beyond the ion range is present in the ^{7}Li relaxation rate profile.

3.3. EPR spectra

Figure 5 shows EPR spectra measured on some selected Xe irradiated LiF samples at two different fields, at 0.333 T (100 and 300 K) and at 14.5 T (at 100 K). The spectra, which do not reveal any temperature or fluence dependence in width or shape, can well be parametrized by a Gaussian line shape with

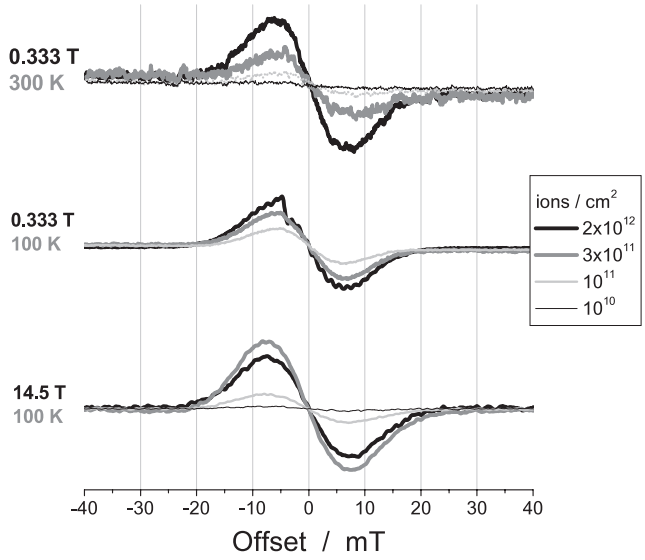

Figure 5. Area normalized EPR spectra (before background correction) for LiF crystals irradiated with Xe fluences as noted in the inset at 0.333 T (100 and 300 K) and 14.5 T (100 K).

intensity $s = s_0(B - B_0)\mathrm{e}^{-\frac{(B-B_0)^2}{\Delta B^2}}$ with a peak-to-peak width ΔB of about 15 mT. Most important for identification is the fact that the width is invariant, even under a change of the Larmor frequency from 9.4 to 406 GHz. From this frequency independence we can infer that the width is due to unresolved hyperfine interactions and that there is no g-factor anisotropy above 3×10^{-4}. This is consistent with the well documented properties of paramagnetic F-centres in irradiated LiF [9]. From the X-band (0.333 T) results an absolute value of the paramagnetic defect concentration could be deduced, which will be discussed in section 3.5. Note that the signal intensity at 14.5 T displays a quite different fluence dependence compared to that of the X-band data: the intensity decreases as the fluence is raised from 3×10^{11} to 2×10^{12} ions cm^{-2}.

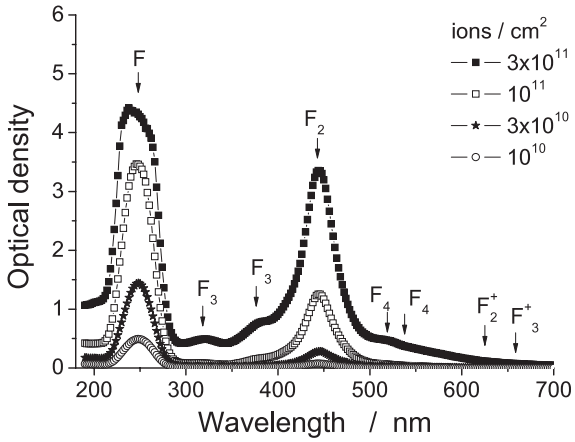

Figure 6. Optical density versus wavelength for LiF crystals exposed to Xe fluences as noted in the inset. The absorption bands of various F_n centres which are marked in the figure are taken from [10–12].

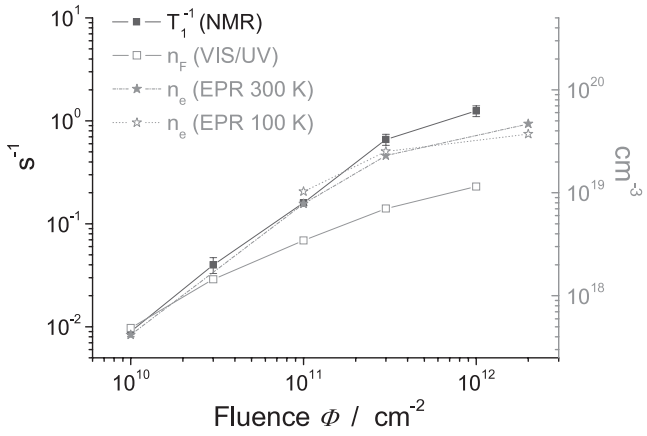

Figure 7. Spin–lattice relaxation rate T_1^{-1} within the ion range, the optically determined concentration of F-centres n_F and the concentration of paramagnetic centres n_e measured at 300 and 100 K by X-band EPR are plotted versus the Xe ion fluence Φ.

3.4. Optical absorption spectra

The results of the absorption measurements are plotted in figure 6. Additionally, the absorption bands of various defects are marked. Since only F, F_2^+ and F_3 centres are paramagnetic, all other defects should not significantly influence the EPR line intensity and the spin–lattice relaxation rate. Even at high fluences no F_2^+ centres can be recognized in the spectra. F_3 centres can be recognized for fluences higher than 3×10^{10} Xe ions cm^{-2}, but their concentration is low compared to the F-centre concentration for all fluences observed.

3.5. Fluence dependence of relaxation rates and paramagnetic centre concentrations

The fluence dependence of the ^{19}F relaxation rates within the ion range, which can be read directly from figure 2, is plotted in figure 7. The figure also contains the fluence dependence of the F-centre concentration (as determined from the optical absorption experiments) as well as that of the total paramagnetic centre concentration (as determined by X-band EPR). It is seen from figure 7 that at low fluences both, T_1^{-1} and the paramagnetic centre concentration, increase approximately linearly with fluence, whereas above a fluence of about 10^{11} ions cm^{-2} there is also a slight tendency towards saturation. In agreement with earlier findings [7], the F-centre concentration evolves towards saturation at much lower fluences.

3.6. F-centres beyond the ion range of an U ion irradiated sample

In order to unravel the origin of the enhanced relaxation rate beyond the ion range (cf figures 2 and 4), we verified the existence of F-centres beyond the ion range by optical absorption spectroscopy: a LiF crystal irradiated with U ions (2.5 GeV; $R = 89.4$ μm; $\Phi = 5 \times 10^{12}$ ions cm^{-2}) was used for estimating the colour centre concentration beyond R induced by ion irradiation. The thickness of the irradiated LiF sample was 2.2 mm. After irradiation a layer of thickness $d_0 \approx$ 110 μm was carefully cleaved from the irradiated surface. The thickness was chosen larger than R to exclude the absorption within the ion range (the longitudinal straggling for 2500 MeV U ions is 2.5 μm [8]). In the remaining crystal, originating from parts of the original crystal completely beyond R, the F-centre area density has been determined by optical absorption spectroscopy (figure 8). The observed absorption beyond the ion range corresponds to a normal irradiation of LiF at a fluence of $\Phi = 5 \times 10^8$ ions cm^{-2} with U ions of the same energy.

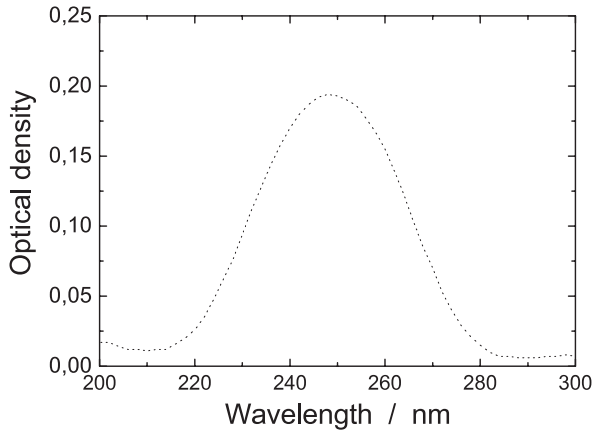

Figure 8. The F-centre absorption beyond the ion track in an irradiated (U ions, $E = 2.5$ GeV, $\Phi = 5 \times 10^{12}$ ions cm^{-2}) LiF crystal. The area density of the created F-centres is equal to $N_F = 1.76 \times 10^{15}$ cm^{-2} and the volume concentration is equal to $n_F = N_F/R = 1.86 \times 10^{17}$ cm^{-3}.

3.7. Increased ^{19}F spin relaxation rate in a Pb ion irradiated but mechanically uncoupled sample

Irradiation with heavy ions is known to induce mechanical stress within the sample [13, 14]. Actually, microhardness and spin–lattice relaxation rate show a similar behaviour beyond the ion range [14]. This motivated the alternative hypothesis that dislocations due to irradiation induced strong internal stresses might be responsible for the enhanced spin–lattice

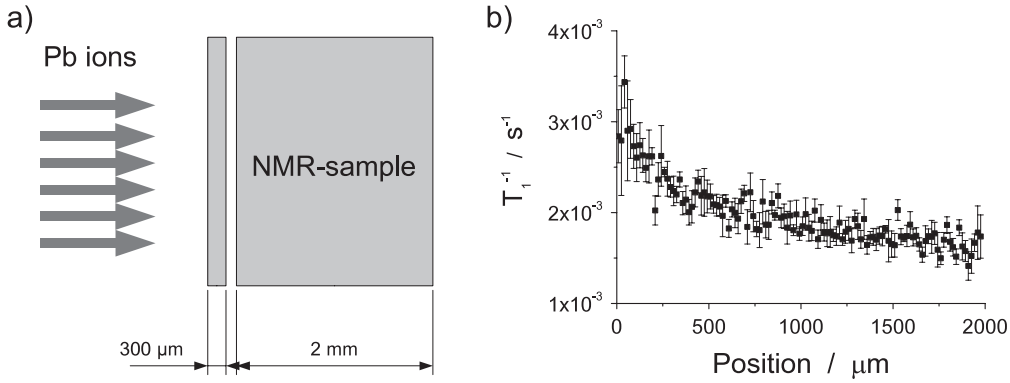

Figure 9. (a) Setting of two mechanically uncoupled LiF crystals for a Pb ion irradiation as indicated. The thickness of the first crystal (300 μm) was assured to be significantly larger than the ion range. (b) Spatially resolved ^{19}F spin–lattice relaxation rate, measured at the second crystal (the right-hand one in (a)) after heavy ion irradiation, as indicated in (a).

relaxation rate. The mechanical coupling of the irradiated and non-irradiated crystal parts would thus directly explain the enhanced relaxation rate beyond the ion range.

Although such dislocations should not cause the observed enhanced relaxation rate as long as they are static, we examined this alternative hypothesis also experimentally.

A LiF crystal was cleaved as indicated in figure 9(a), and the pieces, being arranged one behind the other without mechanical coupling, were exposed in a stack to the ion beam. Due to limited beamtime, the test was restricted to Pb ion irradiation ($E = 1.6$ GeV, $\Phi = 2 \times 10^{12}$ ions cm^{-2}). Then, the second crystal, the one beyond the ion range, was subjected to ^{19}F-NMR microimaging, the relaxation rates being plotted in figure 9(b). Obviously, an enhanced relaxation rate of qualitatively the same kind as seen in figures 2 and 4 appears as well.

3.8. Discussion

We now have to raise the question on the relaxation mechanism in both, (a) the region within the ion range (region 1, <87 μm depth) and (b) beyond it (region 3, >150 μm depth).

(a) Heavy ion irradiation of LiF is known to lead to paramagnetic F-centres which are stable at room temperature: during F-centre formation an anion is moved to an interstitial position and the resulting vacancy is filled by an electron. From optical absorption studies it is well known [7] that a high concentration of paramagnetic F-centres exists in heavy ion irradiated LiF. Indeed, the F-centre concentration deduced from our optical absorption measurements arise in good agreement with these earlier studies. However, as EPR shows (figure 7), F-centres are not the only paramagnetic defects created by heavy ion irradiation. Obviously, the spin–lattice relaxation rate is essentially proportional to the concentration of paramagnetic centres but not to that of F-centres.

Let us compare this result with our expectations from theory: assuming that relaxation is dominated by spin diffusion limited paramagnetic relaxation, the measured rate T_1^{-1} is expected to be proportional to the concentration of paramagnetic centres n_e, i.e. [4]:

$$\frac{1}{T_1} = \frac{8}{3}\pi D_s^{3/4}\left(C\frac{\tau_e}{1+\omega_I^2\tau_e^2}\right)^{1/4} n_e \qquad (1)$$

with $C = (\frac{\mu_0}{4\pi})^2 \frac{2}{5} S(S+1)\gamma_S^2\gamma_I^2\hbar^2$ being the dipolar coupling strength between the nuclear and the electron spins ($S = 1/2$), γ_S and γ_I the electronic and nuclear gyromagnetic ratios, respectively, D_s the ^{19}F spin diffusion coefficient, ω_I the Larmor frequency and τ_e the electron spin relaxation time.

Thus, the experimental finding of $T_1^{-1} \propto n_e$ is consistent with our expectations from theory. But since the F-centre concentration increases more slowly with fluence than the paramagnetic centre concentration, the question about the physical nature of those defects remains. From the optical absorption results in section 3.4 we know that for fluences above 10^{11} ions cm^{-2}, when the ion tracks overlap more and more, significant amounts of complex F_n-centres are produced: diamagnetic F_2- and F_4-centres and paramagnetic F_3-centres. So it is well understood why the F-centre concentration increases sublinearly for fluences $\Phi > 10^{11}$ ions cm^{-2}. However, already at a fluence of 3×10^{11} ions cm^{-2} we find that the F-centre concentration determined optically and the concentration of paramagnetic centres determined by double integration of the X-band spectra differ by approximately a factor of three. The optical absorption spectrum taken at this fluence shows only a relatively small concentration of additional paramagnetic centres, so that complex F_n-centres are unlikely to explain this discrepancy. In the high field EPR spectra, a significant reduction of the intensity of the signal is observed for a fluence of 2×10^{12} ions cm^{-2}. It is noteworthy that no change in line shape is observed over the full fluence range. This reduction in apparent EPR centre density, measured at high field (14.5 T) and high fluence compared to low field (0.333 T) data, might be caused by line broadening as a result of a significant g anisotropy of the as yet unidentified centres created at very high fluence. Further experiments are

necessary to explain the apparent discrepancy between optical absorption spectroscopy and EPR results.

(b) Referring to [8], we can exclude the fact that Xe ions penetrate region 3, the deep crystal interior. Therefore, the enhanced relaxation rate, compared to that in non-irradiated LiF, needs a different explanation. Also from our present finding that the ^{19}F relaxation rate in an irradiated but mechanically uncoupled sample increases (cf section 3.7), we can safely exclude any hypothetical mechanism which involves defects induced by internal stresses caused by the irradiated zone. Also defect diffusion from the zone within the ion range towards the zone beyond can be excluded from this experiment. In [1] we proposed that beyond the ion range the relaxation mechanism is dominated by F-centres which are due to secondary x-rays (bremsstrahlung) from δ electrons generated in the ion tracks. This assumption is now supported by the evidence of F-centres beyond the ion range shown here. Nevertheless, elastic collisions (recoil atoms) and nuclear fragmentation (interaction of the projectile nucleus with the target atom nuclei) [15] may also possibly induce colour centres far beyond the ion range. Further research is needed to single out the dominant mechanism.

4. Conclusions and outlook

Using one-dimensional NMR microimaging we have been able to measure the fluence dependence of the ^{19}F- and (partly) the ^{7}Li-spin–lattice relaxation rates in LiF crystals within, as well as beyond, the ion range. Also, the fluence dependence of the F-centre concentration was measured by optical absorption spectroscopy and that of the total concentration of paramagnetic defects by EPR.

It turns out that the spin–lattice relaxation rate depends linearly on the latter. There is a discrepancy between the optically determined F-centre concentration and that of paramagnetic defects which increase with fluence. This raises questions about the origin of the extra paramagnetic centres. Here, more EPR work (electron spin relaxation rates; unraveling of hyperfine interaction by EPR echo experiments) might be helpful. Also, theoretical work is needed.

As already found in [1] an enhanced relaxation rate is observed beyond the ion range. By irradiating a stack of two mechanically uncoupled crystals and observing enhanced relaxation inside the second crystal (beyond the ion range) internal stresses induced from the irradiated part can be ruled out as a source for relaxation. The physical origin of the defects, among which F-centres have been identified, is not clear. A proposed mechanism involving bremsstrahlung from δ electrons is rather speculative.

Let us finally comment on what can and what will be done in the near future. As the next step, we plan to investigate LiF samples irradiated with different ions (U, Pb, C) for which a different saturation behaviour is expected, corresponding to different track radii. From that we hope to gain information about the fluence dependence of the F-centre density. We also consider irradiation of different types of fluoride crystals. For instance, there exist fluoride crystals where after irradiation the F-centre concentration at room temperature is known to be much lower.

Therefore, it could be easier to observe relaxation processes other than paramagnetic relaxation at F-centres in those crystals.

There is one observation from which an important element of information and a hint for future work can be deduced: from inspection of figure 4 one immediately reads that the ratio $r = T_1^{-1}(^{19}\mathrm{F})/T_1^{-1}(^{7}\mathrm{Li})$ changes as a function of position. Whereas $r \approx 10$ in the irradiated part (region 1), r decreases down to $\approx$3 beyond the ion range (region 3). At present, we do not understand this finding, but it indicates that either the type of defect or the relaxation mechanism changes. In view of this situation, a focus of our future research work will be on experiments which help to unravel the creation process and the physical nature of the paramagnetic centres beyond the ion range.

Acknowledgment

One of us (KPD) acknowledges the hospitality of the Tallahassee high field laboratory which made the reported 406 GHz EPR experiments possible.

References

[1] Stork H, Hamburger A, Gädke A, Fujara F and Schwartz K 2008 *J. Phys.: Condens. Matter* **20** 275236
[2] Klempt T, Schweizer S, Schwartz K, Kanert O, Suter D, Rogulis U and Spaeth J-M 2001 *Radiat. Eff. Defects Solids* **155** 159
[3] Klempt T, Kanert O and Suter D 2003 *Phys. Status Solidi* b **236** 151
[4] Lowe I J and Tse D 1968 *Phys. Rev.* **166** 279
[5] Kimmich R 1997 *NMR Tomography, Diffusometry, Relaxometry* (Heidelberg: Springer)
[6] Perez A, Balanzat E and Dural J 1990 *Phys. Rev.* B **41** 3943
[7] Schwartz K, Trautmann C, El-Said A S, Neumann R, Toulemonde M and Knolle W 2004 *Phys. Rev.* B **70** 184104
[8] Ziegler J F, Ziegler M D and Biersack J P 2006 http://www.srim.org/
[9] Kaplan R and Bray J 1963 *Phys. Rev.* **129** 1919
[10] Perez A, Davenas J and Dupuy C H S 1976 *Nucl. Instrum. Methods* **132** 219
[11] Hughes A E and Jain S C 1979 *Adv. Phys.* **28** 717
[12] Thévenard P, Guiraud G, Dupuy C H S and Delaunay B 1977 *Radiat. Eff.* **32** 83
[13] Manika I, Maniks J and Schwartz K 2008 *J. Phys. D: Appl. Phys.* **41** 074008
[14] Manika I, Maniks J, Schwartz K and Trautmann C 2002 *Nucl. Instrum. Methods* B **196** 299
[15] Czudek J, Jarczyk L, Kamys B, Magiera A, Siudak R, Strzalkowski A and Styczen B 1991 *Phys. Rev.* C **43** 1248